

PCCP

Accepted Manuscript



This is an *Accepted Manuscript*, which has been through the Royal Society of Chemistry peer review process and has been accepted for publication.

Accepted Manuscripts are published online shortly after acceptance, before technical editing, formatting and proof reading. Using this free service, authors can make their results available to the community, in citable form, before we publish the edited article. We will replace this *Accepted Manuscript* with the edited and formatted *Advance Article* as soon as it is available.

You can find more information about *Accepted Manuscripts* in the [Information for Authors](#).

Please note that technical editing may introduce minor changes to the text and/or graphics, which may alter content. The journal's standard [Terms & Conditions](#) and the [Ethical guidelines](#) still apply. In no event shall the Royal Society of Chemistry be held responsible for any errors or omissions in this *Accepted Manuscript* or any consequences arising from the use of any information it contains.

Cite this: DOI: 10.1039/c0xx00000x

www.rsc.org/xxxxxx

ARTICLE TYPE

Water-bath assisted convective assembly of aligned silver nanowire films for transparent electrodes

*Sheng-kai Duan, Qiao-li Niu, Jun-feng Wei, Jie-bing He, Yi-an Yin and Yong Zhang***Received (in XXX, XXX) Xth XXXXXXXXX 20XX, Accepted Xth XXXXXXXXX 20XX*

DOI: 10.1039/b000000x

Abstract: Manipulating Ag nanowire (AgNW) assembly to tailor the opto-electrical properties and surface morphology could improve the performance of the next-generation transparent conductive electrode. In this paper, we demonstrated a water-bath assisted convective assembly process at temporary water/alcohol interface for fabricating hierarchical aligned AgNW electrodes. The convection flow play an important role during the assembly process. The assembled AgNW film fabricated by three orthogonal dip-coating at a water-bath temperature of 80 °C has a sheet resistance of 11.4 Ω/sq with 89.9 % transmittance at 550 nm. Moreover, the root mean square (RMS) of this assembled AgNW film was only 15.6 nm which is much lower than the spin-coated random AgNW film (37.6 nm) with the similar sheet resistance. This facile assembly route provides a new way for manufacturing and tailoring the ordered nanowire-based devices.

Introduction

Due to the emergence of flexible plastic devices and the scarcity of indium resources, finding novel transparent conductive electrode (TCE) materials to replace indium tin oxide (ITO) becomes more urgent. Recent research has focused on several alternatives including conductive polymers,¹ carbon nanotubes,²⁻⁵ graphene,^{6,7} metal grids⁸ and silver nanowires (AgNWs).⁹⁻¹¹ Among them, AgNWs with its high conductivity, excellent flexibility and solution processing have proven to be the most promising candidate alternative to ITO and competing amorphous oxides.¹² AgNW network can be achieved by many means such as spin-coating,^{13,14} drop-casting,^{9,15} rod-coating^{16,17} and spraying-coating.^{18,19} However, the high contact resistance from the loose contact between individual AgNWs and high topological roughness due to AgNWs aggregating remain a critical issue, thus making extra processing steps necessary in order to achieve low sheet resistance values, high transmittance and uniform surface for practical applications. Many strategies have been proposed to address this issue, including mechanical pressing,^{16,20} vacuum filtration,^{12,21} metal-oxide nanoparticle fusing or surface encapsulation,^{22,23} nanoscale joule heating^{24,25} and plasmonic welding process.^{26,27} While concerning rapid production process, some of these methods are time-consuming

and energy-consuming. This suggests a need for tunable, novel and scalable approaches to fabricate AgNW films.

For random AgNW film, the insufficient wire-wire cross junction is also a critical defect. Most of the AgNWs pile up to form high peaks during general random film processes so that a few wire-wire cross junctions are formed with a single AgNW. To overcome this drawback, a layered and aligned AgNW film is required. Metallic nanowire assemblies offer a wide variety of potential applications with improved performance. Many of these assembly techniques have been developed to fabricate the aligned nanowire films. For instance, the Langmuir-Blodgett (LB) technique has been used to align nanowires at the air/water interface by surface compression-assisted and applied in nanoelectronic devices or as sensing substrates for surface-enhanced Raman spectroscopy (SERS).²⁸⁻³⁰ Fluid flows and rheological behavior were employed to direct the nanowires to form well-ordered structures due to the shear flow, and this offered a general pathway for bottom-up assembly of nanosystems.^{31,32} Blown bubble films techniques,³³ dielectrophoretic techniques^{34,35} and stirring-assisted assembly³⁶ have also been introduced to align nanowires. Self-assembly AgNW between two-phase or three-phase (e.g., air/water, water/oil, and oil/water/air) interface recently has also attracted great interest due to their unique structures and potential applications in nanoscale electronics and optoelectronics.³⁷⁻³⁹ Most multi-phase interface assembly reported are focused on an oil/water immiscible interface. Very few studies have been carried out at water/alcohol miscible interface.

In this paper, we report a facile route to fabricate monolayer aligned AgNW film by water-bath assisted convective self-assembly at temporary water/alcohol interface and then transfer these aligned AgNWs onto the glass substrate to form

Laboratory of Nanophotonic Functional Materials and Devices, Institute of Optoelectronic Materials and Technology, South China Normal University, Guangzhou 510631, China

* Address correspondence to zycq@scnu.edu.cn

†Electronic Supplementary Information (ESI) available. See DOI: 10.1039/b000000x/

ordered multilayer AgNW (OM-AgNW) films by dip-coating orthogonally to the previous layer. The thickness, optical transmittance and sheet resistance of OM-AgNW films can be easily tailored by varying the water-bath temperature and the number of dip-coating cycles. The OM-AgNW film from three orthogonal dip-coating at an optimum water-bath temperature of 80 °C exhibited a superior performance of 11.4 Ω/sq sheet resistance and 89.9 % transmittance at 550 nm. The improved performance of OM-AgNW film can be attributed into hierarchical aligned nanowire structure enhancing the number of wire-wire cross junction between nanowires and reducing nanowire aggregation.

Experimental

AgNWs suspension in isopropanol and in water (AW030-L, 1 wt %) were purchased from Kechuang Advanced Materials Technology Co., Ltd. (Hangzhou, Zhejiang, China). The employed AgNWs have an average diameter and length of approximate 25 nm and 20 μm, respectively. In order to minimize agglomerations of AgNWs, the purchased AgNW isopropanol suspension was diluted in isopropanol to form a 0.12 wt % AgNW dispersion. Ultrapure water (resistivity 18.2 MΩcm, Scientecool Co., Ltd.) was added into a glass beaker. Then, the beaker was placed into a water-bath trough and heated. A 150 μL prepared AgNW isopropanol dispersion was added onto the hot water surface drop by drop using a pipette. The location of drop was kept near the center of the water surface to make AgNWs spread out effectively. 1.5×1.5 cm² glass substrates were cleaned with acetone, deionized water and isopropanol each for 10 min in ultrasonic bath. To avoid deposition on the back-sides, two glass substrates were clamped back to back when dip-coating. An automatic dip-coater was used to transfer the assembled film to the glass substrates. A 2000 μm/s pull-out velocity was applied during transferring. Random AgNW films for control group were prepared by multiple times of spin-coating at 1500 rpm with the same diluted AgNW isopropanol dispersion. Both the self-assembled AgNW films and the spin-coated AgNW films were then heated on the hotplate at 100 °C for 5 min to evaporate the remaining solvent.

In the device fabrication, a PEDOT:PSS (Clevis PVP Al 4083) layer was deposited by spin-coating onto the AgNW networks at 2500 rpm for 60 s, and annealed at 120 °C for 10 min. The rest of device fabrication steps were carried out in the nitrogen glove box. A 2 wt % 1:0.8 P3HT:PC₆₁BM (American Dye Source, Inc.) blend from dichlorobenzene was spin-coated onto the PEDOT:PSS layer at 800 rpm for 45 s following a 7 h solvent annealing in a covered Petri dish. After annealing at 120 °C for 10 min, a Ca (20 nm)/Al (100 nm) cathode was thermally deposited at 2×10⁻⁶ Torr. All device areas were 0.15 cm².

The optical transmittance spectra of the films were measured using a UV-vis spectrometer (Agilent Technologies 8453). The surface morphology of the AgNWs was analyzed by a scanning electron microscope (SEM, ZEISS Ultra 55) and atomic force microscopy (AFM, NT-MDT). The sheet resistances of the films were measured by a four-point probe system (KD-1, Kunde Technology Co., Guangzhou, China). Each of the sheet resistances reported is an average value obtained after at least ten multiple measurements. The J-V performance of the devices was

determined by means of a solar simulator (Oriel model 91160) and a Keithley 2400 source measurement unit. All J-V characteristics were obtained in dark and under 100 mW/cm² of AM 1.5 G illumination.

Results and Discussion

Fig. 1a shows the schematic of the self-assembly monolayer AgNW fabrication processes. Fig. 1b-f compares the SEM images of self-assembly monolayer AgNW films fabricated by one dip-coating at room temperature (RT), 50 °C, 70 °C, 80 °C, and 90 °C, respectively. Distinct differences between the self-assembly films with and without water-bath were the surface coverage and alignment of the AgNWs. For room temperature, a random AgNW mesh was formed by dip-coating. The surface coverage of AgNW mesh fabricated at RT was not uniform and AgNWs aggregation can be observed. This is similar to the situation reported by Sachse et al.⁴⁰ A certain scale of ordered AgNW monolayer was obtained when the water-bath temperature came from RT to 50 °C (Fig. 1c). The surface coverage of AgNWs on substrate became uniform and AgNW build-up effect did not occur. The interval of two adjacent AgNWs was reduced and better dense ordered AgNW arrays were formed as the water-bath temperature increased.

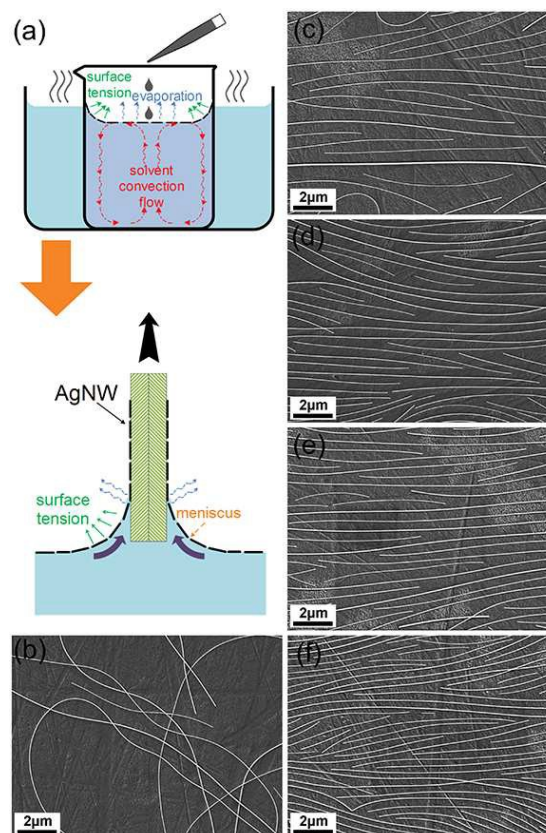


Fig. 1. (a) Schematic illustration of the monolayer AgNW film fabrication on a glass substrate based on water-bath assisted self-assembly by dip-coating. SEM images of the corresponding AgNW monolayer films with the water-bath temperature of RT (b), 50 °C (c), 70 °C (d), 80 °C (e), and 90 °C (f), respectively.

The improvement in the morphology of AgNW monolayer

by water-bath should be attributed to the likelihood of temperature enhancing solvent convection flow-induced AgNW self-assembly. During water-bath heating, the liquid convection circulation has a uprising stream at the center of solvent and down flowing stream near the beaker wall caused by the nonuniform temperature (Fig. 1a). Generally, when a small droplet of an aqueous surfactant is slowly dropped on a thin water surface, the gravitational forces can be neglected and the droplet of the aqueous surfactant will not dissolve into the water immediately but spread first due to the Marangoni effect.⁴¹ In our experiments, the same phenomenon was observed when dropping isopropanol on the water surface. For without water-bath, when dropping AgNW isopropanol dispersion on the water surface, AgNWs quickly sedimentated into the water due to the gravity and the weak nature convective flow though they had the trend to spread (Fig. S1a, initial). As a result, a AgNW water/isopropanol mixed solvent dispersion was formed and became more and more opaque as the number of dropping AgNW dispersion increased (Fig. S1a, final). In contrast, when AgNW isopropanol dispersion was dropped on hot ultrapure water surface, the droplet was not sedimentated immediately but stayed on the water surface and spread out (Fig. S1b, initial). This can be attributed that the uprising stream toward the evaporating liquid surface exerted enough drag of the droplet to overcome the gravity (at least temporarily) and there was enough time for the AgNWs isopropanol dispersion to spread out before sedimentating. During the process, a water/alcohol interface was temporarily formed and the enhanced solvent flow along the water/alcohol surface will drive AgNWs and make them orientate and align due to the shear force caused by the convection flow. AgNWs then gradually self-assembled at the water/air interface as the isopropanol evaporated and appeared as a shiny mirror-like thin interfacial layer (Fig. S1b, final). Finally, the water's high surface tension can allow the self-assembled AgNWs to float on its surface rather than sedimentate with the down flowing stream (Fig. S1b). This solvent flow induced nanowires assembly similar to previous evaporating droplet and convective assembly reported by Michael C.P. Wang et al.⁴² and Huang Y. et al.³¹ As they reported, the movement of a fluid or solid object against a second fluid or solid object can creat a shear force. The orientation of the nanowires dispersion can be realigned by the shear force and the reorientation of the nanowires will be parallel to the direction of the corresponding force. The similarity of our results with those of Huang Y. et al.³¹ indicate that the similar model can be used to explain the assembly of AgNWs here. Therefore, shear forces might be the main force for the initial assembly of the AgNWs at the temporary water/alcohol interface.

The influence of the shear force has been further investigated. In our experiments, when the AgNW isopropanol dispersion was replaced by AgNW water dispersion to drop on the hot water surface, the droplet of AgNW water dispersion sedimentated and redispersed into the water directly and no assembly was observed (Fig. S1c). The same sedimentation has been obtained when dropping the AgNW isopropanol dispersion on hot isopropanol surface (Fig. S1d). In the both two experments, for the homogeneous solvent, weak shear forces were created during dropping process though there was enhanced solvent convection flow in the beaker. Furthermore, the low

surface tension of the isopropanol could not exert enough drag on AgNWs to float on the hot isopropanol surface. Therefore, it could not be assembled to drop the AgNW dispersion on the hot surface of the homogeneous solvent. Other properties such as viscosity, surface tension, boiling point and density maybe have effects on the assembly process. The relative parameters effect on the assembled AgNW film will be further investigated and optimized.

To explain the effect of the water-bath temperature on the performance of monolayer AgNW, absorption spectra of AgNWs from the solvent under the water/air interface have been measured (Fig. 2). The reducing absorption spectra with the increasing water-bath temperature further indicated that the temperature enhancing convection flow contributed to the initial assembly of the AgNWs. As the temperature rised, the droplet would suffer from stronger drag due to the enhanced uprising stream and obtained more time to spread out before sedimentating. Consequently, there were more nanowires self-assembled at the water/air interface. Thus, the number of AgNWs sedimentated into the water would reduce with the increasing of the water-bath temperature. This is consistent with much more coverage and density variation of the aligned AgNWs in Fig. 1c-f.

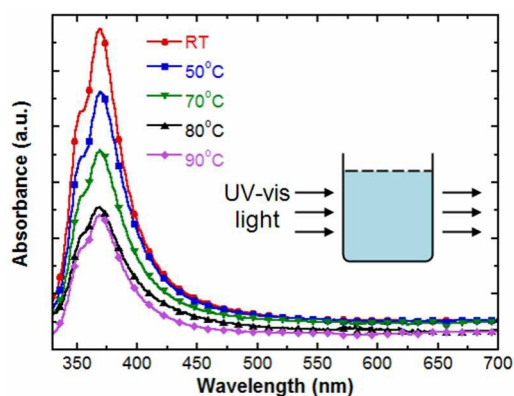


Fig. 2. Absorption spectra of AgNWs from the self-assembly solvents under the water/air interface for the different water-bath temperature.

In consideration of rapid production process of aligned AgNW film, our method is quite flexible and simple. As a result, this method should work as long as the temperature of self-assembly solvent is higher than room temperature. The deposition process was repeated to fabricate layered three-dimensional (3D) crosswire structures simply by rotating the substrate orthogonally to the deposition direction of the previous layer (Fig. 3a). OM-AgNW films have been fabricated to evaluate the optical and electrical properties of such self-assembly AgNW electrodes. In general, the optical transmittance and sheet resistance (R_{sq}) are expressed by⁴³:

$$T(\lambda) = \left(1 + \frac{188.5 \sigma_{Op}(\lambda)}{R_{sq} \sigma_{DC}} \right)^{-2}$$

where σ_{Op} is the optical conductivity and σ_{DC} is the DC conductivity of the film. Transparent electrode is commonly rated by a figure of merit, the ratio of DC to optical conductivity (σ_{DC}/σ_{Op}). A high performance electrode should maintain a low sheet resistance and a high optical transmittance, which

corresponds to a high value of σ_{DC}/σ_{Op} . Fig. 3b compares the optoelectrical performance of OM-AgNW films fabricated at the different water-bath temperatures and number of dip-coating layers. It can be seen that both the sheet resistance and optical transmittance decrease with increasing the dip-coating layer number at the same water-bath temperature or raising the water-bath temperature at the same dip-coating layer number. Transmittance spectra of the corresponding OM-AgNW films are shown in ESI Fig. S2. Figure S3 demonstrated AFM images of the AgNW films with the different layers at the water-bath temperature of 80 °C. The RMS of the corresponding AgNW films increased from 8.2 nm of one layer to 25.4 nm of five layers. More detailed sheet resistances of OM-AgNW films to the different water-bath temperatures and dip-coating layer number are listed in ESI Table S1. For all the self-assembly monolayer AgNW films, sheet resistances were not obtained. This indicates that the same orientation of AgNWs leads to few crosswire junctions between the AgNWs to form a desirable inter-wire conductive path. However, when the substrates were rotated 90° to the deposition direction of last layer and repeated dip-coating, the hierarchical 3D crosswire AgNW structures were achieved, resulting in an enhancement of the contact pathway between nanowires. In addition, for all the AgNW films dip-coated within 5 cycles at RT, no sheet resistance was observed. This may be attributed to non-continuous coverage of the nanowires on the substrates under the room temperature. The values of σ_{DC}/σ_{Op} deduced from the best-fit curves in Fig. 3b improve from 250 to 302 as the water-bath temperature increases from 50 °C to 80 °C.

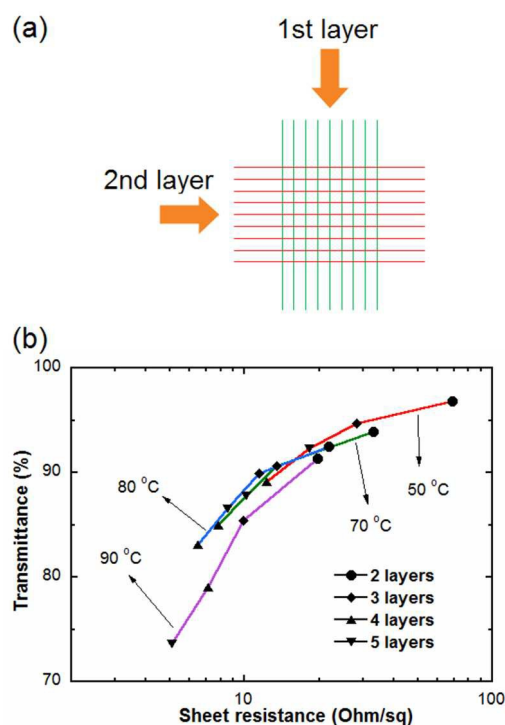


Fig. 3. (a) Transfer of the aligned nanowires onto a substrate to form hierarchical 3D crosswire structures by dip-coating orthogonally to the first deposition direction. (b) Comparison of the opto-electrical performance of the OM-AgNW films from the different water-bath temperatures and dip-coating layer number. However, the value begins to drop at a higher water-bath

temperature such as 90 °C. The higher water-bath temperature results in smaller interval of two adjacent AgNWs. Therefore, more crosswire junctions on AgNWs can be obtained after depositing the follow-up ordered AgNW layers, improving the overall conductivity of the AgNW films. On the other hand, excessively narrow span of two adjacent AgNWs can make the optical transmittance of the AgNW films poor, leading to a relatively lower value of σ_{DC}/σ_{Op} . OM-AgNW film by three orthogonally dip-coating at a water-bath temperature of 80 °C exhibited an optimum sheet resistance of 11.4 Ω/sq and transmittance of 89.9 % at 550 nm.

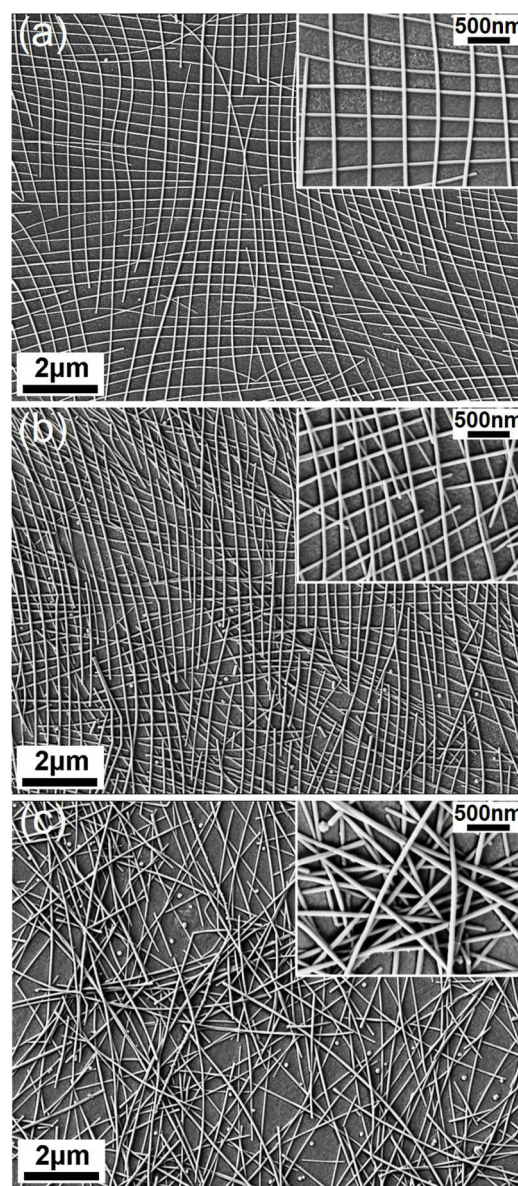


Fig. 4. SEM images of OM-AgNW network of (a) two and (b) three orthogonal dip-coating at the water-bath temperature of 80 °C, and (c) random AgNW network by spin-coating. Insets are their high magnification images.

Fig. 4a and b show the SEM images of OM-AgNW films fabricated by two and three orthogonally dip-coating at 80 °C. As a comparison, shown in Fig. 4c, the random AgNW film was

fabricated by spin-coating and controlled at a similar sheet resistance with the OM-AgNW film fabricated by three orthogonally dip-coating at 80 °C. It can be seen that the coverage of AgNW network is very uniform and ordered after multi-dip-coating deposition. This uniform coverage can enhance wire-wire cross chance and reduce the overall roughness of the film. Hierarchical ordered AgNW structure can make the distribution of wire-wire cross nodes more uniform and form more continuous conductive path relative to random stacking structure. For the spin-coated random AgNW film, nanowires aggregation and stacking have been occurred, leading to less wire-wire cross chance and higher film roughness. In addition, the transmittance of AgNW film by spin-coating is lower than that of OM-AgNW film by dip-coating due to more AgNWs stacking in order to obtain the similar sheet resistance (Fig. 5). The insert of Fig. 5 significantly illustrates AgNWs aggregation at four corners during spin-coating process, resulting in that four corner areas of random AgNW film are darker than the center.

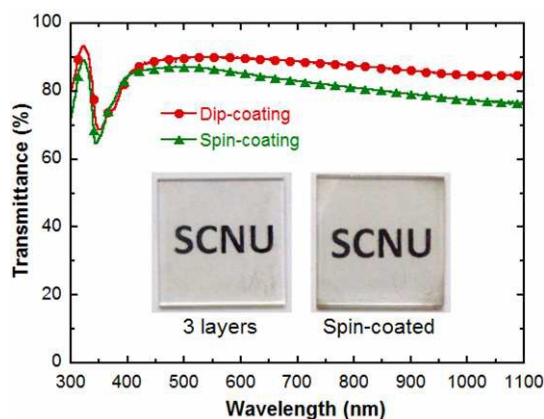


Fig. 5. Transmittance spectra of OM-AgNW film by three orthogonal dip-coating at 80 °C and random AgNW film by spin-coating. The inset illustrates photographs of the corresponding films on 1.5×1.5 cm² glass substrates.

Random AgNW network cannot make full use of each single AgNW to form a large-scale continuous film. As described above, more AgNWs are required to reduce the sheet resistance of random AgNW film to the similar sheet resistance level with OM-AgNW film. Excessive AgNWs result in more AgNWs agglomeration to aggravate optical performance and topography of the AgNW films. Fig. 6a shows a typical atomic force microscopy (AFM) image of the spin-coated AgNW film with $R_{sq}=11.8 \Omega/sq$. The RMS roughness of the film reached 37.6 nm and the peak-to-valley height was about 192 nm, which indicated that there may be seven AgNWs vertical stacking together estimated from the single AgNW with an average diameter of 25 nm. Such high roughness has serious effect on organic device fabrication due to the great risk of shorting between two electrodes in the stack structure. The AFM image of three dip-coated AgNW film with $R_{sq}=11.4\Omega/sq$ was plotted in Fig. 6b. The RMS roughness and peak-to-valley height were significantly reduced to 15.6 nm and 78 nm, respectively, which is consistent with three layer of aligned AgNWs stacking by three dip-coating. This low roughness is very helpful for the electrodes of the organic devices.

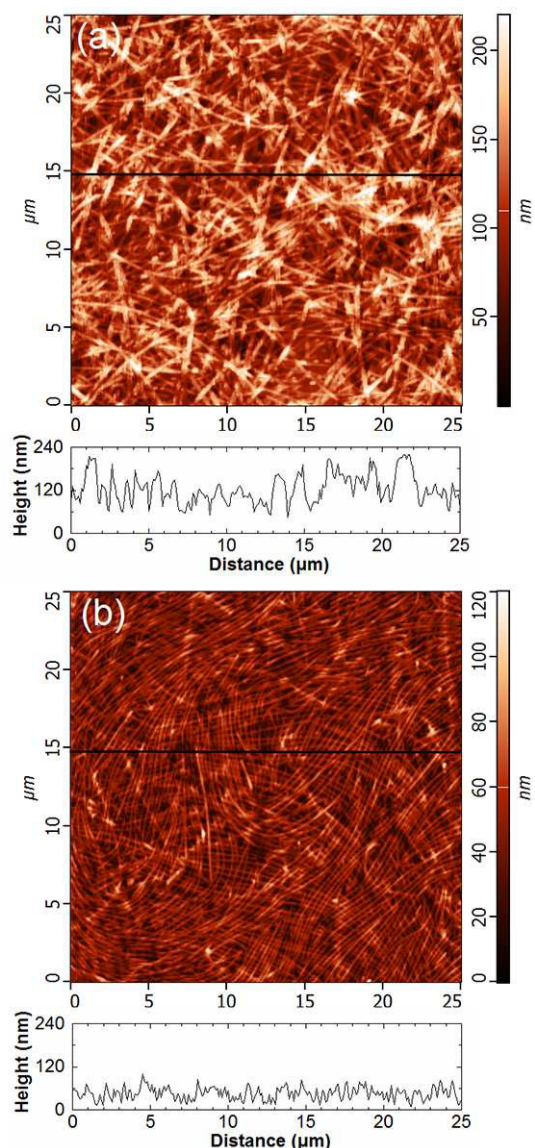


Fig. 6. AFM topographic images of AgNW films by (a) spin-coating and (b) three orthogonal dip-coating at 80 °C. Line profiles along the black lines are shown below the respective AFM images.

In order to investigate the performance for practical application of the OM-AgNW electrodes in organic devices, organic solar cells were fabricated based upon the following architecture: Glass/AgNWs/PEDOT/P3HT:PC₆₁BM/Ca/Al. Fig. 7 shows the current-voltage characteristics of the organic solar cells with random AgNWs and OM-AgNWs as the transparent anodes under 100 mW/cm² of AM 1.5 G illumination and in the dark. It can be seen that the random AgNWs device shows a low short-circuit current density (J_{sc}) and open-circuit voltage (V_{oc}). The random stacking AgNW network fabricated by spin-coating leads to AgNWs tilted out of plane towards the top electrode, suggesting the potential for shorting of the device. However, the J_{sc} and V_{oc} are significantly increased from 7.10 mA/cm² to 9.12 mA/cm² and 0.51 V to 0.58 V for the OM-AgNW anode due to AgNWs mostly parallel to the glass substrate. From the dark J-V curve (Fig. 7b), the shunt resistance was calculated to increase

from $0.47 \text{ k}\Omega\text{cm}^2$ to $8.47 \text{ k}\Omega\text{cm}^2$. The corresponding power conversion efficiency (PCE) was increased from 1.72 % to 2.94 %. We note that the literature reports of devices using similar architecture and ITO as the bottom electrode reached similar efficiencies,^{13,44} demonstrating the applicability of OM-AgNW films as an alternative to ITO.

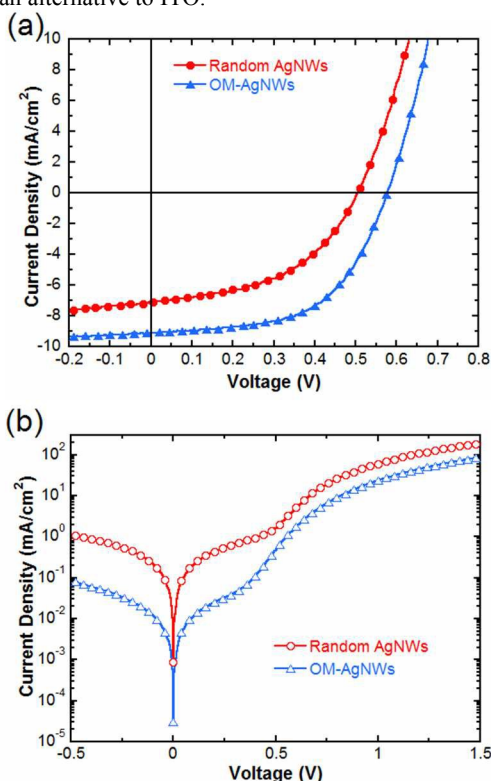


Fig. 7. Current-voltage characteristics of the organic solar cells with random AgNWs and OM-AgNWs as anodes (a) under 100 mW/cm^2 of AM 1.5 G illumination and (b) in dark.

Conclusions

We report a novel and facile approach to fabricate ordered monolayer AgNW film by water-bath assisted convective self-assembly. The introduction of water-bath makes a remarkable difference in manipulating nanowire assembly. The surface coverage of AgNWs on substrate and interval of two adjacent AgNWs can be adjusted by varying the water-bath temperature. Hierarchical aligned AgNW film can be formed simply by repeatedly orthogonal dip-coating process. Optical and electrical properties of the aligned AgNW electrode can be tailored by adjusting the temperature and the deposited layers. Three layer of OM-AgNW film fabricated at a water-bath temperature of $80 \text{ }^\circ\text{C}$ obtained a maximum value of $\sigma_{\text{DC}}/\sigma_{\text{Op}}=302$. RMS of the corresponding AgNW film was only 15.6 nm. Organic solar cells fabricated on this OM-AgNW electrode reached a PCE of 2.94 %. In conclusion, the approach described here has great potential to be generalized to other metal nanowires and a range of plastic substrates for applications beyond organic photovoltaic devices.

Acknowledgements

This work was supported by the Nature Science Foundation of

China (U1174001, 61377065), the Science and Technology Planning Project of Guangdong Province (2012CB010200032), the Science and Technology Project of Guangzhou City (2012J2200023, 2014J4100056), and the Open Fund of the State Key Laboratory of Luminescent Materials and Devices (South China University of Technology).

Notes and references

- M. Vosgueritchian, D. J. Lipomi and Z. N. Bao, *Adv. Funct. Mater.*, 2012, **22**, 421-428.
- M. W. Rowell, M. A. Topinka, M. D. McGehee, H. J. Prall, G. Dennler, N. S. Sariciftci, L. Hu and G. Gruner, *Appl. Phys. Lett.*, 2006, **88**, 233506-233509.
- S. L. Hellstrom, M. Vosguerithian, R. M. Stoltenberg, I. Irfan, M. Hammock, Y. B. Wang, C. Jia, X. Guo, Y. Gao and Z. Bao, *Nano Lett.*, 2012, **12**, 3574-3580.
- C. Feng, K. Liu, J. S. Wu, L. Liu, J. S. Cheng, Y. Zhang, Y. Sun, Q. Li, S. Fan and K. Jiang, *Adv. Funct. Mater.*, 2010, **20**, 885-891.
- Z. Wu, Z. Chen, X. Du, J. M. Logan, J. Sippel, M. Nikolou, K. Kamaras, J. R. Reynolds, D. B. Tanner, A. F. Hebard and et al, *Science*, 2004, **305**, 1273-1276.
- K. S. Kim, Y. Zhao, H. Jang, S. Y. Hee, J. M. Kim, K. S. Kim, J. H. Ahn, P. Kim, J. Y. Choi and B. H. Hong, *Nature*, 2009, **457**, 706-710.
- S. Bae, H. Kim, Y. Lee, X. Xu, J. S. Park, Y. Zheng, J. Balakrishnan, T. Lei, H. R. Kim, Y. I. Song and et al, *Nat. Nanotechnol.*, 2010, **5**, 574-578.
- Y. X. Jin, Y. R. Cheng, D. Y. Deng, C. J. Jiang, T. K. Qi, D. L. Yang and F. Xiao, *ACS Appl. Mater. Interfaces*, 2014, **6**, 1447-1453.
- W. Gaynor, J. -Y. Lee and P. Peumans, *ACS Nano*, 2010, **4**, 30-34.
- C. C. Chen, L. T. Dou, R. Zhu, C. H. Chung, T. B. Song, Y. B. Zheng, S. Hawks, G. Li, P. S. Weiss and Y. Yang, *ACS Nano*, 2012, **6**, 7185-7190.
- Y. X. Jin, D. Y. Deng, Y. R. Cheng, L. Q. Kong and F. Xiao, *Nanoscale*, 2014, **6**, 4812-4818.
- S. De, T. M. Higgins, P. E. Lyons, E. M. Doherty, P. N. Nirmalraj, W. J. Balu, J. J. Boland and J. N. Coleman, *ACS Nano*, 2009, **3**, 1767-1774.
- D. S. Leem, A. Edwards, M. Faist, J. Nelson, D. D. C. Bradley and J. C. de Mello, *Adv. Mater.*, 2011, **23**, 4371-4375.
- J. H. Yim, S. -Y. Joe, C. Pang, K. M. Lee, H. Jeong, J. -Y. Park, Y. H. Ahn, J. C. de Mello and S. Lee, *ACS Nano*, 2014, **8**, 2857-2863.
- Z. B. Yu, Q. W. Zhang, L. Li, Q. Chen, X. F. Niu, J. Liu and Q. B. Pei, *Adv. Mater.* 2011, **23**, 664-668.
- L. B. Hu, H. S. Kim, J. -Y. Lee, P. Peumans and Y. Cui, *ACS Nano*, 2010, **4**, 2955-2963.
- T. Y. Kim, Y. W. Kim, H. S. Lee, H. Kim, W. S. Yang and K. S. Suh, *Adv. Funct. Mater.*, 2013, **23**, 1250-1255.
- A. R. Madaria, A. Kumar and C. W. Zhou, *Nanotechnology*, 2011, **22**, 245201.
- D. Y. Choi, H. W. Kang, H. J. Sung and S. S. Kim, *Nanoscale*, 2013, **5**, 977-983.
- W. Gaynor, G. F. Burkhard, M. D. McGehee and P. Peumans, *Adv. Mater.*, 2011, **23**, 2905-2910.
- P. Lee, J. Lee, H. Lee, J. Yeo, S. Hong, K. H. Nam, D. J. Lee, S. S. Lee and S. H. Ko, *Adv. Mater.* 2012, **24**, 3326-3332.
- R. Zhu, C. H. Chung, K. C. Cha, W. Yang, Y. B. Zheng, H. Zhou, T. B. Song, C. C. Chen, P. S. Weiss, G. Li and et al., *ACS Nano*, 2011, **5**, 9877-9882.
- A. Kim, Y. Won, K. Woo, C. H. Kim and J. Moon, *ACS Nano*, 2013, **7**, 1081-1091.
- H. Tohmyoh and S. Fukui, *Phys. Rev. B*, 2009, **80**, 155403-155407.
- T. -B. Song, Y. Chen, C. -H. Chung, Y. Yang, B. Bob, H. S. Duan, G. Li, K. -N. Tu, Y. Huang, Y. Yang, *ACS Nano*, 2014, **8**, 2804-2811.
- E. C. Garnett, W. S. Cai, J. J. Cha, F. Mahmood, S. T. Connor, M. G. Christoforo, Y. Cui, M. D. McGehee and M. L. Brongersma, *Nat. Mater.*, 2012, **11**, 241-249.
- J. Lee, J. Y. Woo, J. T. Kim, B. Y. Lee and C. -S. Han, *ACS Appl. Mater. Interfaces* 2014, **6**, 10974-10980.
- A. Tao, F. Kim, C. Hess, J. Goldberger, R. R. He, Y. G. Sun, Y. N. Xia and P. D. Yang, *Nano Lett.*, 2003, **3**, 1229-1233.

- 29 D. Whang, S. Jin, Y. Wu and C. M. Lieber, *Nano Lett.*, 2003, **3**, 1255-1259.
- 30 A. R. Tao, J. Huang and P. D. Yang, *Acc. Chem. Res.*, 2008, **41**, 1662-1673.
- 5 31 Y. Huang, X. F. Duan, Q. Q. Wei and C. M. Lieber, *Science*, 2001, **291**, 630-633.
- 32 H. Zhou, P. Heyer, H.-J. Kim, J.-H. Song, L. H. Piao and S.-H. Kim, *Chem. Mater.*, 2011, **23**, 3622-3627.
- 33 G. H. Yu, A. Y. Cao and C. M. Lieber, *Nat. Nanotechnol.*, 2007, **2**, 372-377.
- 10 34 T. I. Lee, W. J. Choi, K. J. Moon, J. H. Choi, J. P. Kar, S. N. Das, Y. S. Kim, H. K. Baik and J. M. Myoung, *Nano Lett.*, 2010, **10**, 1016-1021.
- 35 E. M. Freer, O. Grachev, X. F. Duan, S. Martin and D. P. Stumbo, *Nat. Nanotechnol.*, 2010, **5**, 525-530.
- 15 36 W. Z. Li, W. Wei, J. Y. Chen, J. X. He, S. N. Xue, J. Zhang, X. Liu, X. Li, Y. Fu, Y. H. Jiao and et al, *Nanotechnology*, 2013, **24**, 105302-105307.
- 37 J. W. Liu, H. W. Liang and S. H. Yu, *Chem. Rev.*, 2012, **112**, 4770-4799.
- 20 38 S. Y. Zhang, J. W. Liu, C. L. Zhang and S. H. Yu, *Nanoscale*, 2013, **5**, 4223-4229.
- 39 H. Y. Shi, B. Hu, X. C. Yu, R. L. Zhao, X. F. Ren, S. L. Liu, J. W. Liu, M. Feng, A. W. Xu and S. H. Yu, *Adv. Funct. Mater.*, 2010, **20**, 958-964.
- 25 40 C. Sachse, L. Müller-Meskamp, L. Bormann, Y. H. Kim, F. Lehnert, A. Philipp, B. Beyer and K. Leo, *Org. Electron.*, 2013, **14**, 143-148.
- 41 K. S. Lee and V. M. Starov, *J. Colloid Interf. Sci.*, 2009, **329**, 361-365.
- 30 42 M. C. P. Wang and B. D. Gates, *Mater. Today*, 2009, **12**, 34-43.
- 43 D. S. Hecht, L. Hu and G. Irvin, *Adv. Mater.*, 2011, **23**, 1482-1513.
- 44 D. Angmo and F. C. Krebs, *J. Appl. Polym. Sci.*, 2013, **129**, 1-14.